

# Single-Crystal Magic-Angle Spinning $^{17}\text{O}$ NMR and Theoretical Studies of the Antiferroelectric Phase Transition in Squaric Acid<sup>†</sup>

N. S. Dalal,<sup>\*,‡,§</sup> K. L. Pierce,<sup>‡,||</sup> J. Palomar,<sup>‡,||</sup> and R. Fu<sup>§</sup>

Department of Chemistry and Biochemistry, and National High Magnetic Field Laboratory, Florida State University, Tallahassee, Florida 32306-4390, and Departamento de Química Física Aplicada, Universidad Autónoma de Madrid, Spain

Received: September 11, 2002; In Final Form: December 12, 2002

We report resolution-enhanced magic-angle sample spinning (MAS)  $^{17}\text{O}$  NMR studies of the paraelectric–antiferroelectric phase transition (at  $T_C = 373$  K) of the model hydrogen-bonded compound squaric acid ( $\text{H}_2\text{C}_4\text{O}_4$ ). Utilization of single crystals in the MAS measurements yielded a factor of 4 decrease in the  $^{17}\text{O}$  NMR line widths, as compared to powder samples. All four oxygens were clearly shown to be chemically different at  $T < T_C$ . This was akin to  $^{13}\text{C}$  spectra, but the  $^{17}\text{O}$  peaks are much more dispersed. The peak assignment was supported by quantum theoretical calculations of the  $^{17}\text{O}$  isotropic chemical shifts using a pentamer model of the crystal structure below  $T_C$ . On raising the temperature, the four peaks merged and became a narrow doublet above  $T_C$ , in contrast to a singlet for  $^{13}\text{C}$ . Also, the mean position of the doublet was not the average of the four low-temperature peaks. This observation suggests that the phase transition involves a distortion of the whole  $\text{H}_2\text{C}_4\text{O}_4$  framework, and not just the order–disorder rearrangement of the H's i.e., future models of the transition should include a displacive component, in addition to an order–disorder part. The observation of the doublet at  $T > T_C$  implies that the two O–H...O chains retain their difference in the paraelectric phase as well. This is consistent with the one-dimensional Ising chain model, according to which the SQA lattice should be visualized as a mesh of two distinct and orthogonal one-dimensional chains, in contrast to the more prevalent two-dimensional  $\text{C}_4\text{O}_4$  square-lattice model.

## 1. Introduction

Many hydrogen-bonded solids exhibit cooperative phenomena, such as structural phase transitions, accompanied by anomalous changes in many thermodynamic, dielectric, and lattice-dynamical properties whose underlying (atomic level) mechanism is generally not well understood.<sup>1–4</sup> An example of such materials is the simple organic compound squaric acid, 1,2-dihydroxy-3-cyclobutene-3,4-dione,  $\text{H}_2\text{C}_4\text{O}_4$ , henceforth SQA, whose structure is shown in Figure 1. In this work we report on a very high resolution, variable temperature,  $^{17}\text{O}$  NMR investigation of the paraelectric–antiferroelectric phase transition in SQA at its  $T_C$  of 373 K.<sup>1</sup> The phase transition involves mainly the localization of the H's in the O–H...O bonds which hold the lattice together as essentially a two-dimensional sheet of  $\text{C}_4\text{O}_4$  squares, held together in three dimensions by weak van der Waals forces. At  $T > T_C$ , SQA has an average  $C_{4h}$  symmetry, with the H's occupying positions, on a statistical basis, at the middle of the O–H...O bonds. At  $T < T_C$ , the H's are locked close to one or the other O's, the symmetry is thus lowered and the unit cell acquires an antiferroelectric configuration of the electric dipoles on the  $\text{H}_2\text{C}_4\text{O}_4$  units in the lattice. Since the discovery of its phase transition, SQA has been studied theoretically<sup>5–9</sup> as well as experimentally, including by tech-

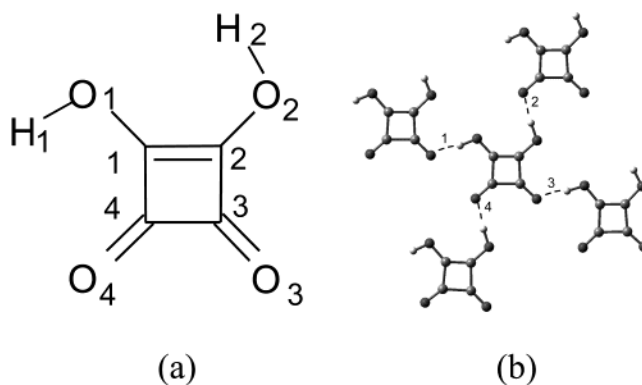


**Figure 1.** Structure of squaric acid: (a) skeleton (b) a hydrogen-bonded pentamer.

niques such as X-ray<sup>1,10</sup> and neutron diffraction,<sup>4,11,12</sup> infrared<sup>13–15</sup> and Raman scattering,<sup>16,17</sup> and solid-state NMR<sup>18–22</sup> and NQR.<sup>23</sup> In particular, high-resolution solid-state NMR measurements have proven to be uniquely helpful for investigating the structure, dynamics, and the nature of this phase transition.<sup>24–28</sup> However, much of the earlier work has focused on the role of the C and H sites; and the role of the O atoms has remained pretty much unexplored. The exception is the  $^{17}\text{O}$  NQR study by Seliger et al.,<sup>23</sup> whose major result was that the low-temperature phase persists up to about 20 K above  $T_C$ . One of the reasons for the lack of the experimental data on the oxygen is that it is the naturally (>99%) abundant isotope,  $^{16}\text{O}$ , has its nuclear spin  $I = 0$ , and is thus NMR-inactive. With a view to help remove this constraint, in the present study we have explored the potential of magic-angle sample spinning

<sup>†</sup> Part of the special issue “George S. Hammond & Michael Kasha Festschrift”.

\* Corresponding author.

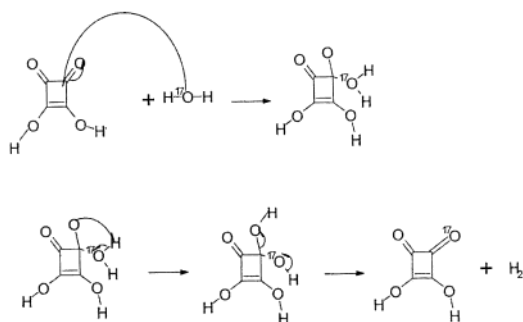
<sup>‡</sup> Department of Chemistry and Biochemistry, Florida State University.

<sup>§</sup> National High Magnetic Field Laboratory, Florida State University.

<sup>||</sup> Universidad Autónoma de Madrid.

<sup>‡</sup> Current address: Department of Chemistry, University of California, Berkeley, Berkeley, CA 94720.

## SCHEME 1



(MAS) NMR methodology,<sup>29,30</sup> utilizing the  $^{17}\text{O}$  isotropic chemical shift as the probe in the study of the phase transition in SQA. Because of the inherently very low signal-to-noise ratio of  $^{17}\text{O}$  NMR (natural abundance 0.037%,  $I = 5/2$ ), our measurements were made possible by using  $^{17}\text{O}$ -labeled samples, especially single crystals. The use of single crystals improved the spectral resolution by a factor of 4 (at least), which enabled us to observe some  $T_C$ -related changes in the spectral features that were not observable via the standard (powder) MAS measurements.

The initial impetus for the current study arose from the fact that the mechanism of the paraelectric–antiferroelectric phase transition in SQA is still controversial. While much of the earlier work has been discussed in terms of a two-dimensional order–disorder model, recent evidence from neutron diffraction<sup>4</sup> and  $^{13}\text{C}$  NMR data<sup>9</sup> has suggested that the mechanism must involve the order–disorder behavior of protons in two distinct, and practically independent, one-dimensional (1-D) hydrogen-bonded  $\text{HO}-\text{C}=\text{C}-\text{C}=\text{O}$  chains. Thus, the thermally induced flipping of the  $\text{H}_2$  proton (see Figure 1 for notation), which is part of the more conjugated hydrogen-bonded chain,<sup>9</sup> might be considered as the first step in the initiation of the phase transition. This step implies a pseudorotation of the molecule of  $90^\circ$  and the interchanging of the role of the  $\text{H}_2$  and  $\text{H}_1$  protons. Consecutive pseudorotations along the two diagonal coordinates would result in a disordered structure below  $T_C$ . The other, more basic and unsolved question is whether the transition can be described as a pure order–disorder type, with the proton dynamics playing the primary role, or whether displacive features, related to the concomitant distortion of the  $\text{C}_4\text{O}_4$  unit, must also be taken into account, as stressed in a previous report based on our  $^{13}\text{C}$  NMR measurements and theoretical modeling.<sup>28</sup> The present study is an attempt to answer at least a significant part of these questions, based on both our  $^{17}\text{O}$  NMR and quantum mechanical calculations of the NMR data.

## 2. Experimental and Computational Details

**2.1.  $^{17}\text{O}$  Labeling.** Squaric acid was purchased from Sigma and used as received. The  $^{17}\text{O}$  labeling was accomplished by heating the dissolved compound in about 20%  $^{17}\text{O}$ -labeled  $\text{H}_2\text{O}$ , in a closed vessel. The labeled water was obtained from Isotec. Both the labeled water and squaric acid were refrigerated until used. The mechanism for the isotopic exchange can be simply rationalized as described in Scheme 1.

The isotope labeling was confirmed by mass spectrometry, and was found to be about 15% (exact number not critical to this study), sufficient for the NMR signal detection within a few minutes. The  $T_C$  of the labeled sample was determined to be 372 K by independent specific heat measurements in our laboratory, using a Quantum Design PPMS Model 6000, with temperature accuracy of about 0.05 K.

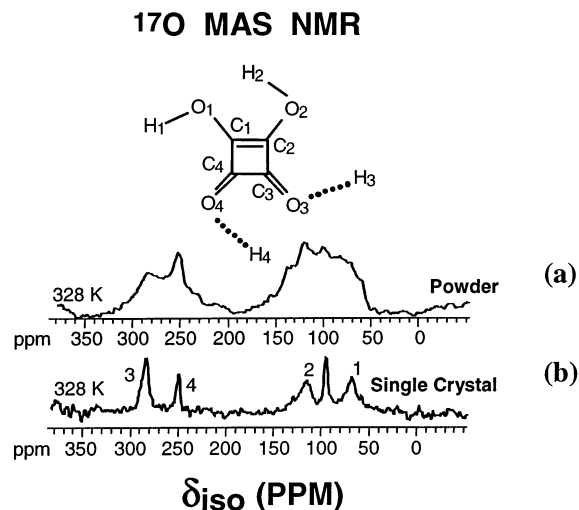


**Figure 2.**  $^{17}\text{O}$  MAS NMR spectra of the central ( $1/2 \rightarrow -1/2$ ) transition of a  $^{17}\text{O}$ -labeled SQA in the form of (a) powder; (b) single crystal. Note the narrower peaks in (b). The peak numbering corresponds to that in Figure 1. The sharp line at 105 ppm corresponds to a spinning sideband.

**2.2. NMR Measurements.** The  $^{17}\text{O}$  magic-angle spinning (MAS) measurements were made using a Bruker 600 MHz wide-bore solid-state NMR spectrometer available at the National High Magnetic Field Laboratory. The  $^{17}\text{O}$  resonance frequency was close to 81 MHz, with the sample spinning at 12.5 kHz. The variable temperatures were achieved by nitrogen gas flow, and controlled to within 0.1 K. The sample temperature was checked using the  $^{13}\text{C}$  NMR procedure, based on the phase transition itself, as described previously.<sup>22, 24–26</sup> Both powders and single crystals were used in the study; the crystal providing narrower lines by a factor of about four. Spectra were accumulated at 10 K intervals from 300 to 350 K, above which the temperature interval was reduced to 1 K, until about 10 K above the  $T_C$  (372 K).

**2.3. Computational Method.** The molecular geometry of the isolated SQA molecule and the pentamer cluster have been obtained using the B3LYP method<sup>32,33</sup> in conjunction with a 6-31G\*\* basis set. To avoid the interaction effects between the surrounding SQA units, the two-dimensional pentamer structure was optimized fixing the hydrogen-bond angles given by neutron diffraction data at 15 K,<sup>4</sup> but leaving free the rest of coordinates. The details of the geometric optimization and related considerations have been reported recently.<sup>9</sup> The isotropic NMR nuclear shieldings ( $^{17}\text{O} \sigma_{\text{iso}}$ ) were calculated at the B3LYP/6-31G\*\* level using the GIAO<sup>34,35</sup> method. All computations were performed with the aid of the Gaussian 98 program.<sup>36</sup>

The conversion to chemical shifts ( $^{17}\text{O} \delta_{\text{iso}}$ ) was done using the experimental–theoretical linear correlation obtained from the current results of SQA. Predicted  $^{17}\text{O}$  chemical shifts for the couples  $\text{O}_1/\text{O}_4$  and  $\text{O}_2/\text{O}_3$  obtained as  $^{17}\text{O} \delta_{\text{iso}}(\text{O}_1/\text{O}_4) = X_{\text{H}_1}(70/250) + (1 - X_{\text{H}_1})(250/70)$  and  $^{17}\text{O} \delta_{\text{iso}}(\text{O}_2/\text{O}_3) = X_{\text{H}_2}(115/285) + (1 - X_{\text{H}_2})(285/115)$ , where  $X_{\text{H}_1}$  and  $X_{\text{H}_2}$  are the experimental proton occupancies from ref 4, or the double well potential occupancies below  $T_C$  from ref 37.

## 3. Results and Discussion

**3.1. Resolution Enhancement from MAS Using Single Crystals.** Figure 2 shows some typical  $^{17}\text{O}$  NMR spectra from  $^{17}\text{O}$ -labeled samples of SQA powder (Figure 2a) and a single crystal (Figure 2b) in the low-temperature phase ( $T < T_C$ ). It is seen that both the powder and the crystal show four distinct peaks, marked 1, 2, 3, and 4 in light of the numbering in Figure

**TABLE 1: Comparison of Calculated NMR Chemical Shifts from the Theoretical SQA Models with the Experimental Data by High-Resolution Solid-State NMR Spectroscopy**

	$^{17}\text{O}$ NMR			$^{13}\text{C}$ NMR <sup>b</sup>		
	isolated <sup>a</sup>	pentamer <sup>a</sup>	expt	isolated	pentamer	expt
O <sub>1</sub>	65	89	70	184.2	187.1	187.0
O <sub>2</sub>	77	95	115	186.9	187.8	187.7
O <sub>3</sub>	324	270	285	187.6	192.9	193.9
O <sub>4</sub>	311	261	250	193.1	195.0	194.3

<sup>a</sup> Experimental-theoretical linear correlation:  $^{17}\text{O} \delta_{\text{iso}} = 209 - 0.64 \text{ } ^{17}\text{O} \sigma_{\text{iso}}$  (Sd = 25 ppm, R = 0.983).

1. The remaining peak(s) in Figure 2 are the spinning sidebands, as was verified by the fact that their relative positions change in proportion to the spinning frequency. The observed peaks fall under two distinct sets: the more shifted peaks around 250 ppm can be assigned to the carbonyl ( $>\text{C}=\text{O}$ ) oxygens, while the less-shifted doublet (around 100 ppm) can be assigned to the  $>\text{C}-\text{O}-\text{H}$  hydroxyl oxygens, in analogy with the earlier reported  $^{13}\text{C}$  peaks from SQA.<sup>24–28</sup> Further support for this assignment was provided by our theoretical calculations, as discussed in the following subsection.

Another noteworthy observation from Figure 2 is that the peaks in Figure 2b (single crystal) are narrower by at least a factor of 4 as compared to those in Figure 2a (powder). The mechanism of this effect is not understood at this point. At first it appeared to be related to the reduction of the anisotropic bulk magnetic susceptibility (ABMS) broadening, as described in general by Van der Hart et al.<sup>29</sup> However, the powder spectra did not exhibit a significantly narrowing on dispersion of the sample in silica, as would be the case if ABMS were the cause. This question thus remains open at this time.

One can also note the much higher sensitivity of the  $^{17}\text{O}$  NMR to the effect of the proximity of the H, as compared to that of the  $^{13}\text{C}$ , for this type of hydrogen-bonded system. For SQA, the splitting within a doublet is about 30 ppm for  $^{17}\text{O}$ , but only about 1 ppm in the case of  $^{13}\text{C}$ .<sup>24–28</sup> This extra dispersion enabled us to follow the phase transition in a much more precise manner (vide infra) than was possible with  $^{13}\text{C}$ .

### 3.2. Computational NMR Analysis and Peak Assignments.

As a first step in understanding the chemical shifts of SQA, we calculated the  $^{17}\text{O}$  NMR parameters of the isolated (i.e., gas-phase) SQA molecule, obtained by the GIAO method at the B3LYP/6-31G\*\* level. The calculations yield four significantly different  $^{17}\text{O}$  chemical shifts for the gas-phase compound (Table 1).

Clearly, this result implies that the electronic environment (bonding) is distinctly different around each oxygen fragment of the asymmetric SQA ring. As expected, the two carbonyl oxygens show much higher  $^{17}\text{O}$  chemical shifts than the hydroxyl oxygens.

Significantly, the  $^{17}\text{O}$  NMR signals corresponding to the O<sub>2</sub> and O<sub>4</sub> oxygen atoms included in the more conjugated  $\text{H}_2-\text{O}_2-\text{C}_2=\text{C}_1-\text{C}_4=\text{O}_4$  chain are located in the middle of the spectra (Figure 3).

These results are in contrast to the  $^{13}\text{C}$  chemical shift order found previously,<sup>9</sup> in which a lower  $^{13}\text{C}$  shielding was found for C<sub>2</sub> and C<sub>4</sub>, as compared to C<sub>1</sub> and C<sub>3</sub>. These findings are explainable on the basis that the resonance along the  $\pi$ -conjugated double bond system leads to an increase of the electron density around the carbonyl oxygen and conversely a deshielding of the hydroxyl oxygen as well as to some extent both carbon atoms.

For a more realistic comparison of the theory with the  $^{17}\text{O}$  NMR measurements, we extended the calculations to a pentamer

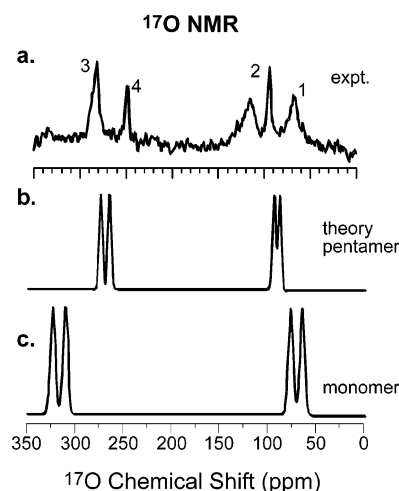
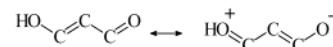


**Figure 3.** (a) Typical solid-state  $^{17}\text{O}$  MAS NMR spectra of a SQA single crystal; (b) theoretically calculated  $^{17}\text{O}$  NMR spectrum for SQA using the pentamer model; and (c) theoretically calculated  $^{17}\text{O}$  NMR spectrum for isolated molecule of SQA by the GIAO-B3LYP/6-31G\*\* method.

### SCHEME 2



structure, as shown in Figure 1b, that includes a fairly complete hydrogen-bonding network surrounding an SQA molecule. The pentamer model, optimized at the B3LYP/6-31G\*\* level, has been shown to predict reasonably well the structural parameters from neutron diffraction measurements.<sup>9</sup> In addition, we found that for the pentamer case the calculated  $^{13}\text{C}$  NMR data reproduced the experimental results, allowing an accurate assignment of the spectral peaks.<sup>9</sup> On the basis of these results, we compare in Table 1 the experimental CP/MAS spectra of single SQA crystal with the  $^{17}\text{O}$  chemical shifts for the central molecule of the pentamer calculated by the GIAO//B3LYP-6-31G\*\* method. Clearly, the computationally predicted  $^{17}\text{O}$  NMR spectrum presents four peaks associated with the four different oxygen atoms (Figures 2 and 3). Indeed, the peaks at 70 and 285 ppm can be assigned, respectively, to O<sub>1</sub> and O<sub>3</sub> atoms, whereas those at 115 and 250 ppm are those from O<sub>2</sub> and O<sub>4</sub>. The pentamer results also show that the effect of hydrogen-bonding is to increase the  $^{17}\text{O} \delta_{\text{iso}}$  values of hydroxyl oxygen atoms and to decrease those of the carbonyl ones. These results can be simply attributed to the increasing contribution of the resonance to the two  $\text{H}-\text{O}-\text{C}=\text{C}=\text{O}$  systems by the hydrogen-bond interactions (Scheme 2).

**3.3. Temperature Dependence of  $^{17}\text{O}$  NMR Spectra.** A major goal of this undertaking was to probe the possible change in the electronic structure of the oxygen sites as the sample temperature is varied across the  $T_c$ . Figure 4 shows the temperature dependence of the spectra in the paraelectric phase (above  $T_c$ ) as well as in the antiferroelectric phase, below  $T_c$ . On increasing the temperature the peaks move toward each other as  $T \rightarrow T_c$  from the low-temperature side. At higher temperatures, close to  $T_c$ , the peak separation decreases, and within about 2 K of the  $T_c$ , they merge to a narrow doublet with about 10 ppm separation (Figure 5). It is noteworthy that the location of this doublet is *not* the average of the four low-temperature peaks; this point is discussed in detail in the following section. We tried several crystal orientations in the MAS experiments with the view of eliminating the crystal orientation effect, but could never get the double splitting to lower than about 5–10 ppm.

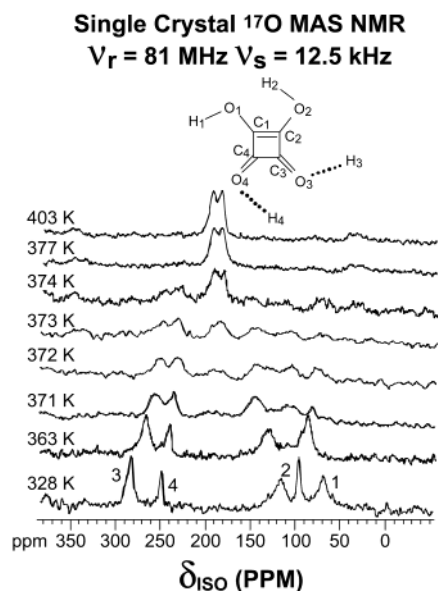


**Figure 4.** Temperature dependence of  $^{17}\text{O}$  MAS NMR spectra of single-crystal SQA.

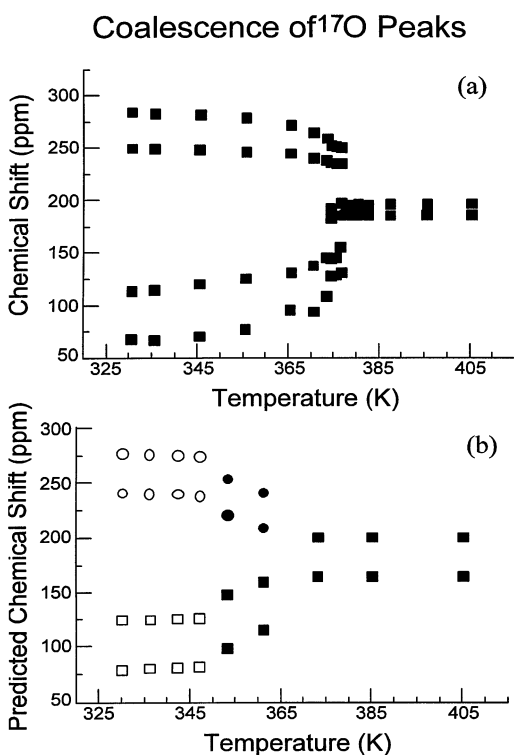


**Figure 5.** (a) Temperature dependence of  $^{17}\text{O}$  chemical shifts of SQA obtained by solid-state high-resolution NMR measurements; (b) predicted  $^{17}\text{O}$  chemical shifts for the couples  $\text{O}_1/\text{O}_4$  and  $\text{O}_2/\text{O}_3$  obtained applying the temperature-dependent site occupancies for hydrogen atoms as fractional functions of the carbonyl and hydroxyl contributions to  $^{17}\text{O}$  NMR signals.

This was also then verified by MAS measurements on powder samples (Figure 6).

As can be noted from Figure 6a, a doublet splitting of a similar magnitude is found also for the powder samples. Hence we conclude that the splitting is not an artifact of crystal orientation in the MAS measurements. Disregarding the actual amount of this doublet separation, it is important to note that the presence of this doublet at  $T$  well above  $T_c$ , rather than a singlet, implies two different electronic environments for the oxygen atoms in the paraelectric phase, i.e., it is direct evidence

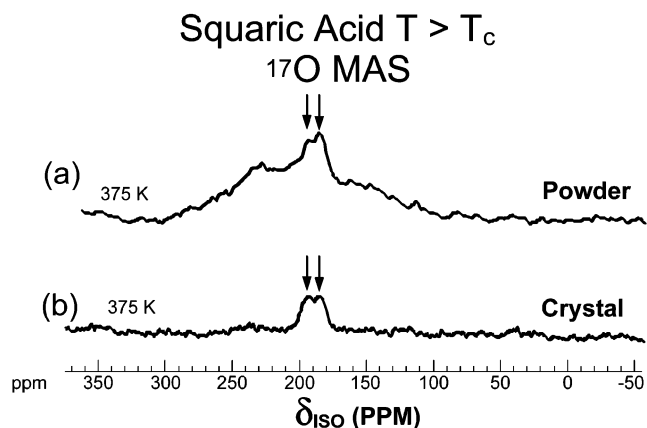


**Figure 6.** Comparison of  $^{17}\text{O}$  MAS spectra of SQA at  $T > T_c$ : (a) powder, (b) single crystal. The arrows highlight the doublet structure of the motionally averaged peak. See text for its significance.

that the structure of SQA at temperatures up to  $T_c$  actually is a dynamic average of the low ( $C_2$ )-symmetry structures made possible by placing the H's in two different O-H...O bonds. It may also be noted that the doublet structure persists to at least 20 K above the  $T_c$ . One another finding is that the  $T_c$  observed here from  $^{17}\text{O}/^{18}\text{O}$  samples and MAS NMR measurements coincides essentially with that determined via  $^{13}\text{C}$  NMR spectroscopy,<sup>24–28</sup> and also with the original birefringence data.<sup>3</sup> This is in contrast to earlier reported  $^{17}\text{O}$  NQR results,<sup>23</sup> that detected the low-symmetry to high-symmetry change at about 20 K above the thermodynamic  $T_c$ . The underlying reason for this discrepancy might be related to the time-scale of the present NMR vs NQR techniques, but this seems unlikely and needs further examination. Finally, there is the interesting observation in Figure 3 that over a few degree range around  $T_c$ , signals from the paraelectric and antiferroelectric phases are simultaneously present. This is reminiscent of what was found in the earlier  $^{13}\text{C}$  NMR studies,<sup>24–26</sup> and is consistent with the fact that the SQA phase transition is complex: it is essentially of the first order, but exhibits some features of a second-order type.

The above-discussed peak coalescence is reminiscent of a similar observation of peak coalescence in our earlier  $^{13}\text{C}$  chemical shift data.<sup>9</sup> This can be understood by invoking a time averaging statistical contribution from a carbonyl and a hydroxyl group with different hydrogen-bond environments of the partially disordered SQA structure. This was similar to the pseudorotation mechanism proposed for the proton motion by Semmingsen et al.<sup>4</sup> Applying this hypothesis to the case of  $^{17}\text{O}$  NMR, the environments of  $\text{O}_2$  and  $\text{O}_4$  after the proton flip of  $\text{H}_2$  should correspond closely to those of the ordered  $\text{O}_3$  and  $\text{O}_1$  sites, respectively. In addition, the initial  $\text{O}_1$  and  $\text{O}_3$  gradually obtain  $\text{O}_4$  and  $\text{O}_2$  character, respectively, through such  $+90^\circ$  pseudorotation. In Figure 5 we present the  $^{17}\text{O}$  chemical shift of SQA obtained applying the refined site occupancies for the hydrogen atoms, obtained at different temperatures,<sup>4</sup> (and also the occupation probabilities of the double-well potential given Samuelsen et al.<sup>37</sup>) as fractional function of the carbonyl and hydroxyl contributions to the  $^{17}\text{O}$  chemical shifts. We observe that the pseudorotational model predicts the emergence of two peaks in the middle zone of the  $^{17}\text{O}$  NMR spectra above  $T_c$ , supporting the postulate that the two chains of the compound retain their difference at  $T > T_c$ .

**3.4. Temperature Dependence of the Average Value of  $^{17}\text{O}$  Peaks.** An important objective of this study was to assess

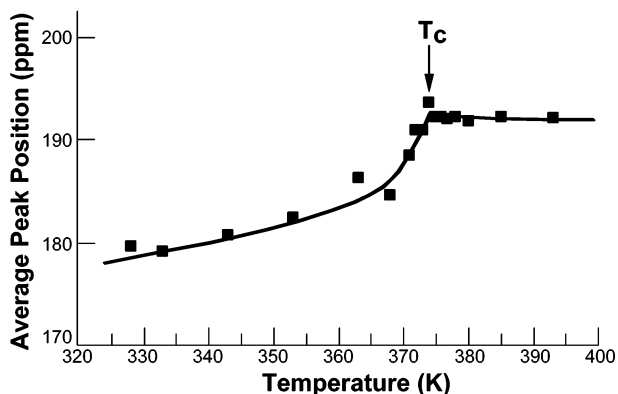


**Figure 7.** Temperature dependence of the average  $^{17}\text{O}$   $\delta_{\text{ISO}}$  in the close vicinity of the paraelectric–antiferroelectric phase transition of SQA.

whether the transition mechanism involves only the order–disorder behavior of the H's or if it involves also some displacive contribution, as discussed earlier in connection with the  $^{13}\text{C}$  data.<sup>24–28</sup> This was accomplished by measuring the change in the shift obtained by averaging the positions of all the peaks in going through the phase transition. The basic idea here is that the parameter  $\delta_{\text{ISO}}$  is a sensitive function of the overall electronic structure, and is invariant to any rotational or translational change in the molecule.<sup>20,24</sup> Thus if the phase transition were of the pure order–disorder type, then the average  $\delta_{\text{ISO}}$  should remain virtually unchanged when the sample temperature is varied across the phase transition. Any anomalous change in  $\delta_{\text{ISO}}$  for a given atomic site would imply that the transition involves a change in the electronic structure at the  $T_c$ . Such an observation is considered qualitative evidence for the presence of a displacive character in the mechanism of the phase transition.<sup>20, 24</sup>

Figure 7 shows the temperature dependence of the averaged value of  $\delta_{\text{ISO}}$  for all four oxygens in SQA. Even when the broadening of the peaks leads to some dispersion of the data, we can note that the average  $\delta_{\text{ISO}}$  increases steadily as  $T \rightarrow T_c$ , and exhibits an anomalous increase of about 13 ppm within 2–3 K of the  $T_c$ . It is thus seen that the high-temperature position of  $^{17}\text{O}$   $\delta_{\text{ISO}}$  is different from that expected from the motional averaging of the four low-temperature peaks. This result implies that the chemical structure in the paraelectric phase is not just a time-average of the various low symmetry forms, but must include a definitive change in molecular geometry. The transition mechanism must thus involve both an order–disorder and a displacive component.

#### 4. Summary and Conclusions

Summarizing, this study yielded two major results. First, in cases such as the hydrogen-bonded solid studied here, MAS using single crystals can afford several times higher resolution than obtained through the more routine procedure of using powdered samples. The present study constitutes, to our knowledge, the first report of such resolution enhancement for  $^{17}\text{O}$ . Additionally, relative to  $^{13}\text{C}$ , the  $^{17}\text{O}$  nucleus affords a factor of nearly 5 higher spectral resolution. Second, the observation of four clearly resolved  $^{17}\text{O}$  NMR peaks at  $T < T_c$  constitutes a direct evidence of the presence of two different hydrogen-bonded Ising chains in SQA. The detection of a doublet rather

than a singlet at  $T > T_c$ , together with the fact that the higher temperature peaks are not at the algebraic average of the four low-temperature signals, implies that the transition mechanism consists of both an order–disorder and a displacive component. We thus believe that this study will stimulate significant new theoretical as well as experimental investigations.

**Acknowledgment.** This research was supported in part by a grant from the National Science Foundation and Florida State University. We acknowledge Centro de Computación Científica of Universidad Autónoma de Madrid for the computer time.

#### References and Notes

- (1) Semmingsen, D. *Tetrahedron Lett.* **1973**, *11*, 807.
- (2) Samuelsen, E. J.; Semmingsen, D. *Solid State Commun.* **1975**, *17*, 217.
- (3) Semmingsen, D.; Feder, J. *Solid State Commun.* **1974**, *15*, 1369.
- (4) Semmingsen, D.; Tun, Z.; Nelms, R. J.; McMullan, R. K.; Koetzele, T. F. Z. *Kristallogr.* **1995**, *210*, 934, and references therein.
- (5) Rostkowska, H.; Nowak, M. J.; Lapinski, L.; Smith, D.; Adamowicz, L. S. *Spectrochim. Acta A* **1997**, *53*, 959.
- (6) Zhou, L.; Zhang, Y.; Wu, L.; Li, J. *J. Mol. Struct. (Theochem.)* **2000**, *497*, 137.
- (7) Spassova, M.; Kolev, T.; Kanev, I.; Jacquemin, D.; Champagne, B. *J. Mol. Struct. (Theochem.)* **2000**, *528*, 151.
- (8) Rovira, C.; Novoa, J.; Ballone, P. *J. Chem. Phys.* **2001**, *115*, 6406.
- (9) Palomar, J.; Dalal, N. S. *J. Phys. Chem. B* **2002**, *106*, 4799.
- (10) Semmingsen, D. *Acta Chem. Scand.* **1973**, *27*, 3961.
- (11) Semmingsen, E.; Hollander, F. J.; Koetzele, T. F. *J. Chem. Phys.* **1977**, *66*, 4405.
- (12) Hollander, F. J.; Semmingsen, D.; Koetzele, T. F. *J. Chem. Phys.* **1977**, *67*, 4825.
- (13) Bougeard, D.; Novak, A. *Solid State Commun.* **1978**, *27*, 453.
- (14) Moritomo, Y.; Koshihara, S.; Tokura, Y. *J. Chem. Phys.* **1990**, *93* (8), 5429.
- (15) Moritomo, Y.; Katsufuji, T.; Tokura, Y. *J. Chem. Phys.* **1991**, *95* (4), 2244.
- (16) Samuelsen, E. J.; Semmingsen, D. *J. Phys. Chem. Solids* **1977**, *38*, 1275.
- (17) Ehrhardt, K. D.; Buchenau, U.; Samuelsen, E. J.; Maier, H. D. *Phys. Rev.* **1984**, *B29*, 996.
- (18) Blinc, R.; Burger, M.; Rutar, V.; Seliger, J.; Zupancic, I. *Phys. Rev. Lett.* **1977**, *38*, 92.
- (19) Mehring, M.; Suwaleck, D. *Phys. Rev. Lett.* **1979**, *42*, 317.
- (20) Mehring, M.; Becker, D. *Phys. Rev. Lett.* **1981**, *47*, 366.
- (21) Kuhn, W.; Maier, H. D.; Petersson, J. *Solid State Commun.* **1979**, *32*, 249.
- (22) Maier, H. D.; Muser, H. E.; Petersson, J. *Z. Phys. B* **1982**, *46*, 251.
- (23) Seliger, J.; Zagar, V.; Blinc, R. *J. Magn. Reson.* **1984**, *58*, 359.
- (24) Klymchyov, A. N.; Dalal, N. S. *Z. Phys. B* **1997**, *104*, 651.
- (25) Klymchyov, A. N.; Dalal, N. S. *Solid State Nucl. Magn. Reson.* **1997**, *9*, 85.
- (26) Klymchyov, A. N.; Dalal, N. S. *Ferroelectrics* **1998**, *206–207*, 103.
- (27) Fu, R.; Klymchyov, A. N.; Bodenhausen, G.; Dalal, N. S. *J. Phys. Chem.* **1998**, *102*, 8732.
- (28) Dalal, N. S.; Klymchyov, A. N.; Bussmann-Holder, A. *Phys. Rev. Lett.* **1998**, *81*, 5924.
- (29) Van der Hart, D. L.; Earl, W. L.; Garroway, A. N. *J. Magn. Reson.* **1981**, *44*, 361.
- (30) Fyfe, C. A. *Solid State NMR for Chemists*; CRC Press: Boca Raton, FL, 1984.
- (31) Palomar, J.; Klymchyov, A. N.; Panizian, D.; Dalal, N. S. *J. Phys. Chem. A* **2001**, *105*, 8926.
- (32) Becke, A. D. *J. Chem. Phys.* **1993**, *98*, 5648.
- (33) Lee, C.; Yang, W.; Parr, R. G. *Phys. Rev. B* **1988**, *37*, 785.
- (34) Dietchfield, R. *Mol. Phys.* **1974**, *27*, 789.
- (35) Wolinski, K.; Hilton, J. F.; Pulay, P. *J. Am. Chem. Soc.* **1990**, *112*, 8251.
- (36) Frisch, M. J., et al. *Gaussian 98*; Gaussian, Inc.: Pittsburgh, PA, **1998**.
- (37) Samuelsen, E. J.; Buchenau, U.; Dieter, M.; Ehrhardt, K.; Fjaer, E.; Grimm, H. *Phys. Scr.* **1982**, *25*, 685.